Application Note

Assessment of drug-induced liver toxicity

A case study with trovafloxacin and levofloxacin in a human liver-on-chip model

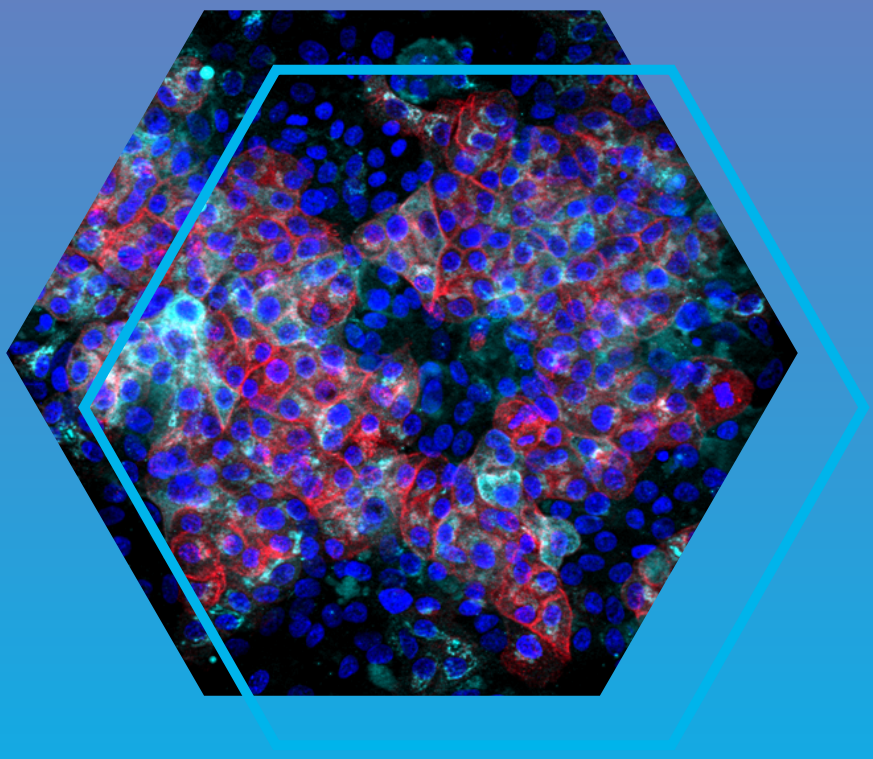

Author:
Tim Kaden

Release date:
14/10/2024

Important - please read

It is important to note that due to donor variability, monocyte-derived macrophages (MDMs) from different donors may exhibit variations in their response to different drug compounds. Consequently, this variability among different biological replicates should be considered in the interpretation of experimental results.

Abstract

Drug-induced liver injury (DILI) poses a significant risk to patient safety, often leading to drug withdrawals and considerable financial losses for the pharmaceutical industry. While traditional preclinical models such as simple 2D cell cultures and animal models still have limitations in detecting DILI, microphysiological chip-based models are a powerful tool to detect such adverse events. Such tools, also called organ-on-chip models, mimic the physiological microenvironment of the organ, using human cells for a more precise clinical evaluation. This application outlines a case study using a human microphysiological liver model to assess DILI of two fluoroquinolones, trovafloxacin (TVX) and levofloxacin (LVX). This model incorporates expandable human liver sinusoidal endothelial cells (LSECs), monocyte-derived macrophages (MDMs), and differentiated HepaRG hepatocytes, thereby reflecting the correct microanatomy and physiological complexity of the human liver. Trovafloxacin, already withdrawn from the market due to high DILI concerns, induced significant vascular and hepatocellular toxicity, unlike the structurally related, approved and non-toxic LVX. The findings demonstrated in this application underscore the value of the liver model in enhancing the detection of DILI during preclinical testing, potentially improving drug safety evaluation and reducing the risk of adverse events in clinical settings.

Highlights

- The liver model described is a promising tool to evaluate DILI in a human-relevant context and can validate the hepatotoxic profile of TVX and the non-toxic profile of LVX in a more sensitive way compared to 2D monocultures.
- The model is particularly suitable to measure clinical-relevant hepatotoxicity markers, such as vascular and hepatic tissue injury, cell viability, LDH and ALT release, and secretion of inflammatory cytokines. These parameters are elevated in models treated with clinical concentrations of TVX.
- The safety profile of LVX is confirmed even at concentrations above applied clinical concentrations.
- TVX-induced DILI involves glutathione depletion and mitochondrial-associated reactive oxygen generation, providing crucial insights into the toxicity mechanism of the drug.

Introduction

Drug-induced liver injury (DILI) remains a significant challenge in drug development, especially as it can lead to acute liver failure in patients and is a common reason for drug withdrawals (Stevens & Baker, 2009; Watkins, 2011). Antimicrobials, including fluoroquinolone antibiotics like trovafloxacin (TVX), are frequently associated with DILI (Andrade et al., 2005; Chalasani et al., 2015). While TVX has been withdrawn from the market due to severe hepatotoxic effects (Ball et al., 1999), the structural analogue levofloxacin (LVX) is generally considered safe with scarce reports of liver toxicity (De Sarro & De Sarro, 2001). However, accurately predicting drug toxicity remains difficult in preclinical stages, as animal models often fail to accurately replicate human liver responses due to interspecies differences (Olson et al., 2000; Butler et al., 2017). To address this issue, a microphysiological human liver model (Rennert et al., 2015) designed to mimic key aspects of human liver function, including vascular perfusion, was leveraged to evaluate the hepatotoxicity of TVX and LVX at clinically relevant concentrations. We demonstrated that TVX induces significant liver injury, inflammation, glutathione depletion, and mitochondrial dysfunction, while LVX did not elicit comparable effects. Moreover, TVX-induced disruption of cell viability was more prominent in the liver model compared to 2D monocultures, highlighting the improved sensitivity in detecting DILI. The model can be used as a platform to screen various drug candidates of interest and to investigate their related toxicity mechanisms in detail. Prospectively, the model holds potential for improving early-stage drug safety testing and reducing the risk of DILI in clinical trials.

Materials and Methods

The materials and methods outlined in this application note closely follow those outlined in Kaden et al. 2023. Any modifications or adaptations made to the protocol are clearly specified.

Peristaltic pump

(can be purchased in line with the DynamicOrgan System)

DynamicOrgan Developers Kit

Including:
/ Biochips (BC002)
/ 2-Stop Tubing
/ Connectors (Adapter)
/ Reservoirs

Cells

Differentiated HepaRG cells
Upcyte liver sinusoidal endothelial cells (LSECs)
Monocyte-derived macrophages (MDMs)

Media and reagents

Endothelial cell growth medium (ECGM MV) + supplements
Vascular perfusion medium (VPM): M199 medium + supplements
Hepatic thawing and seeding medium (HTSM): William's Medium E + CM3000 + supplements
Hepatic perfusion medium (HPM): William's Medium E + CM4000 + supplements

Results

1. The liver-on-chip model for evaluation of DILI

BC002, a Dynamic42 biochip, containing an integrated polyethylene-terephthalate (PET) membrane with randomly distributed pores (median density: $1 \times 10^5/cm^2$) of 8 µm in diameter was used as a platform to build the liver model. Human expandable liver sinusoidal endothelial cells (LSECs) were seeded in the top channel (Figure 1) and were statically cultured for 5 days. After reaching confluency, monocyte-derived macrophages (MDMs) as surrogates for Kupffer cells were seeded on top of the LSECs. Differentiated HepaRG hepatocytes were seeded in the bottom channel on the opposite side of the membrane as a hanging layer. Up to this point, the biochips were maintained under static conditions. Two days after seeding the HepaRG cells, perfusion of the top channel including LSECs and MDMs was initiated using a peristaltic pump. The appropriate medium was circulated from a microfluidic reservoir through the vascular channel in a circular-loop system, with daily medium exchange. The bottom channel harboring the HepaRG cells remained under static conditions with daily medium exchange. The liver models were pre-perfused for 24 hours until drug treatment was applied. Liver models were treated for up to 7 days with the respective drugs diluted in vascular perfusion medium (VPM).

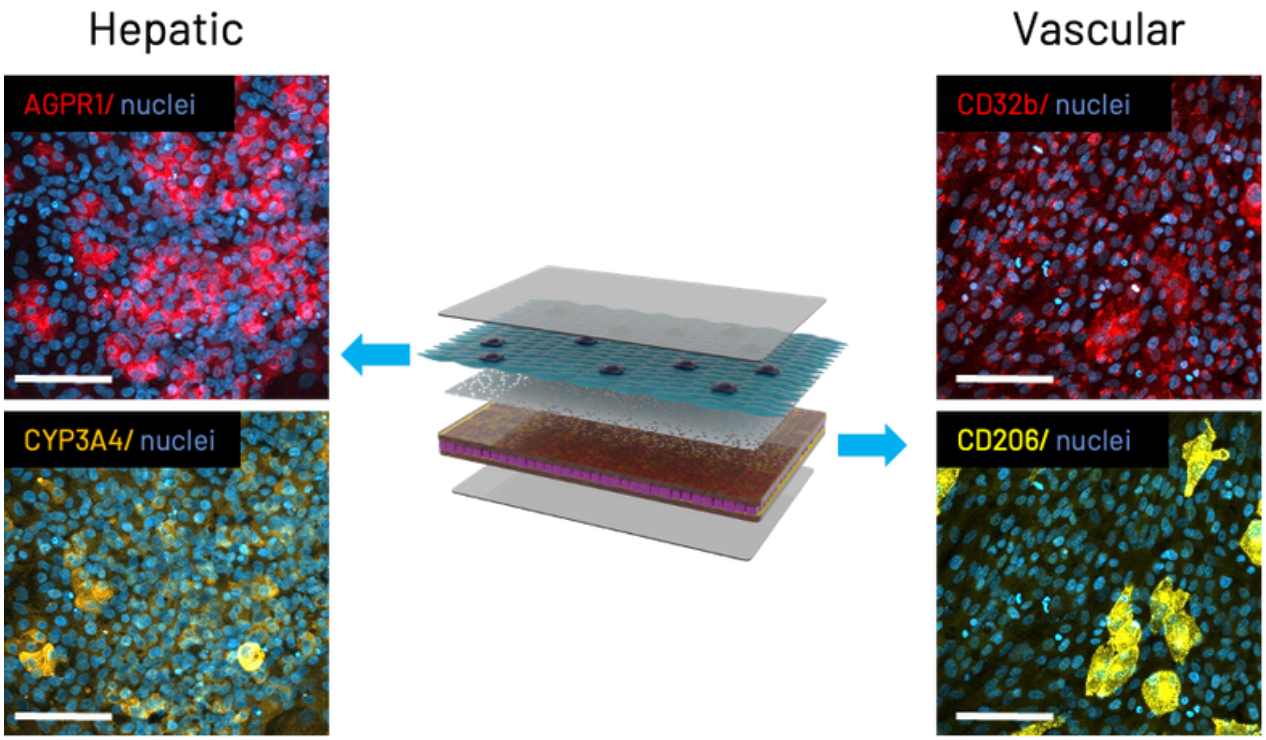

Figure 1: Representative immunofluorescence staining of: left panel: hepatic cell layer stained for asialoglycoprotein receptor 1 (ASGPR1, red) and cytochrome P450 3A4 (CYP3A4, orange); mid-panel: 3D view of vascular cell layer including endothelial cells (blue) and macrophages (purple) and the hepatic cell layer consisting of hepatocytes (magenta/brown); right panel: vascular cell layer stained for Fc Gamma Receptor IIb (CD32b, red) and mannose receptor (CD206, yellow); Scale bars = 100µm.

2. Comparison of tissue damage in treated liver models and 2D monocultures

Liver models were treated with different concentrations of TVX, LVX, and staurosporine (positive damage control) for 7 days. TVX treatment induced a concentration-dependent cytotoxic effect, reducing DAPI-positive nuclei and cellular viability in both hepatic and vascular channels (Figure 2 A). TVX treatment at 10 µM and 20 µM significantly reduced nuclei counts in both hepatic and vascular layers (Figure 2B-C), highlighting its cytotoxicity compared to LVX, which caused minimal reductions only at the highest concentration tested. In 2D HepaRG cultures, TVX also led to a concentration-dependent reduction in viability (Figure 2D), mostly reflecting results in 3D models. TVX primarily damaged HepaRG cells in 2D cultures, while no toxic effects were demonstrated in 2D cultured LSECs. LVX had no significant impact on cell viability in either 2D or 3D models. These findings show the improved sensitivity of the liver model in revealing both hepatic and vascular toxicity of TVX.

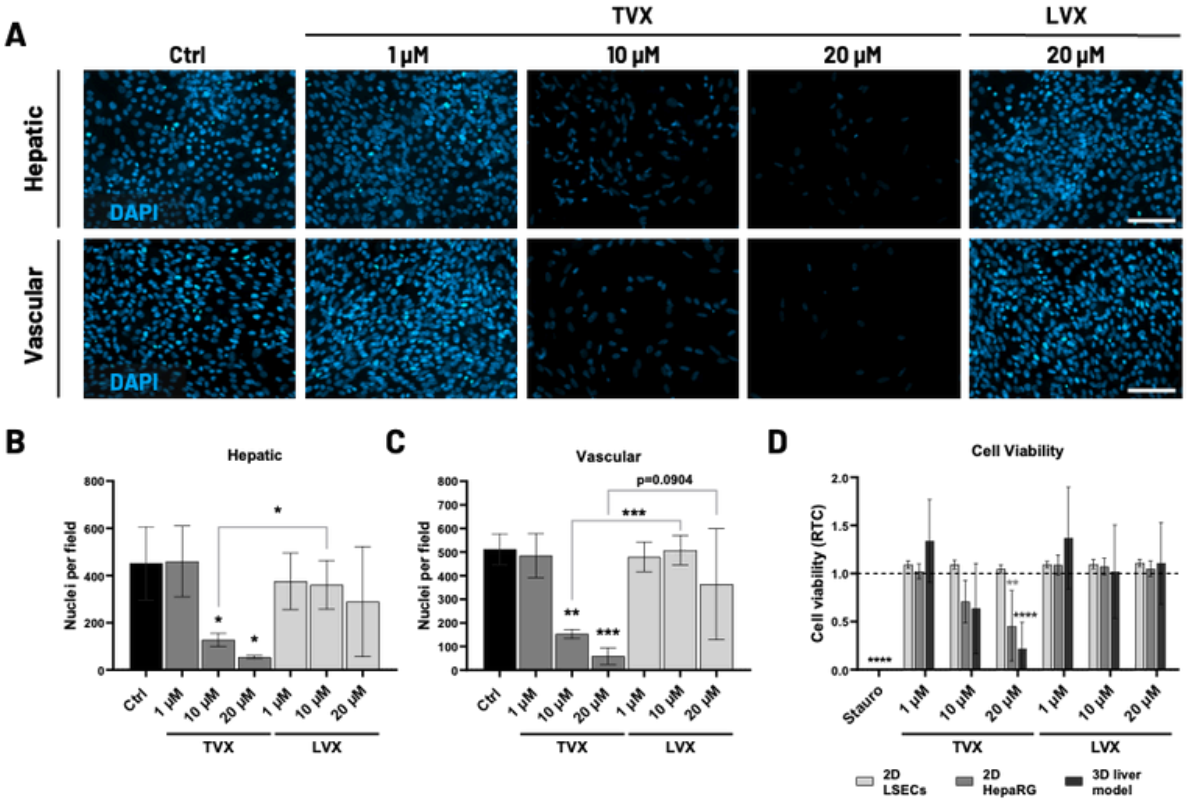

Figure 2: Assessment of tissue injury and cell viability. A) Representative fluorescence images of liver models after 7 days of treatment with: control (Ctrl, 0.1% DMSO), TVX at 1 µM, 10 µM, 20 µM and LVX at 20 µM for 7 days. Cell nuclei from hepatic and vascular layers were stained for DAPI (blue). Scale bars, 100 µm. B-C) Quantification of nuclei counts per image in hepatic (B) and vascular (C) cell layers after 7 days of treatment. Bars represent mean ± SD of 3 independent experiments (n = 3 chips with 5 randomly selected membrane regions for each condition). *p ≤ 0.05, **p ≤ 0.01, ***p ≤ 0.001 (Two-way ANOVA with Tukey's multiple comparison test (1 B-C). D) Measurement of cellular viability in 2D cultured HepaRG cells, LSECs, and 3D liver models. Viability assay performed with 2D cultures or liver models treated with control (Ctrl, 0.1% DMSO), 10 µM staurosporine (Stauro), TVX and LVX at a concentration of 1 µM, 10 µM or 20 µM for 7 days. Cell viability was measured as relative light units (RLU). Bars represent mean plotted as ratio to control (RTC, dotted baseline) ± SD of at least 3 independent experiments (n ≥ 3). **p ≤ 0.01, ****p ≤ 0.0001 (One-way ANOVA with Dunnett's multiple comparison test, two-tailed t test for comparison between indicated conditions.

3. Examination of fluorescence marker expression and morphology in drug-treated liver models

After 7 days of daily treatment with TVX and LVX, liver models were analyzed for vascular and hepatic tissue morphology using immunofluorescence staining. TVX, particularly at concentrations of 10 µM and 20 µM, caused significant vascular injury, as shown by reduced cell nuclei and decreased expression of CD32b and CD206 in LSECs and MDMs (Figure 3 A-B). In contrast, LVX had no impact on vascular morphology or fluorescence signal intensities.

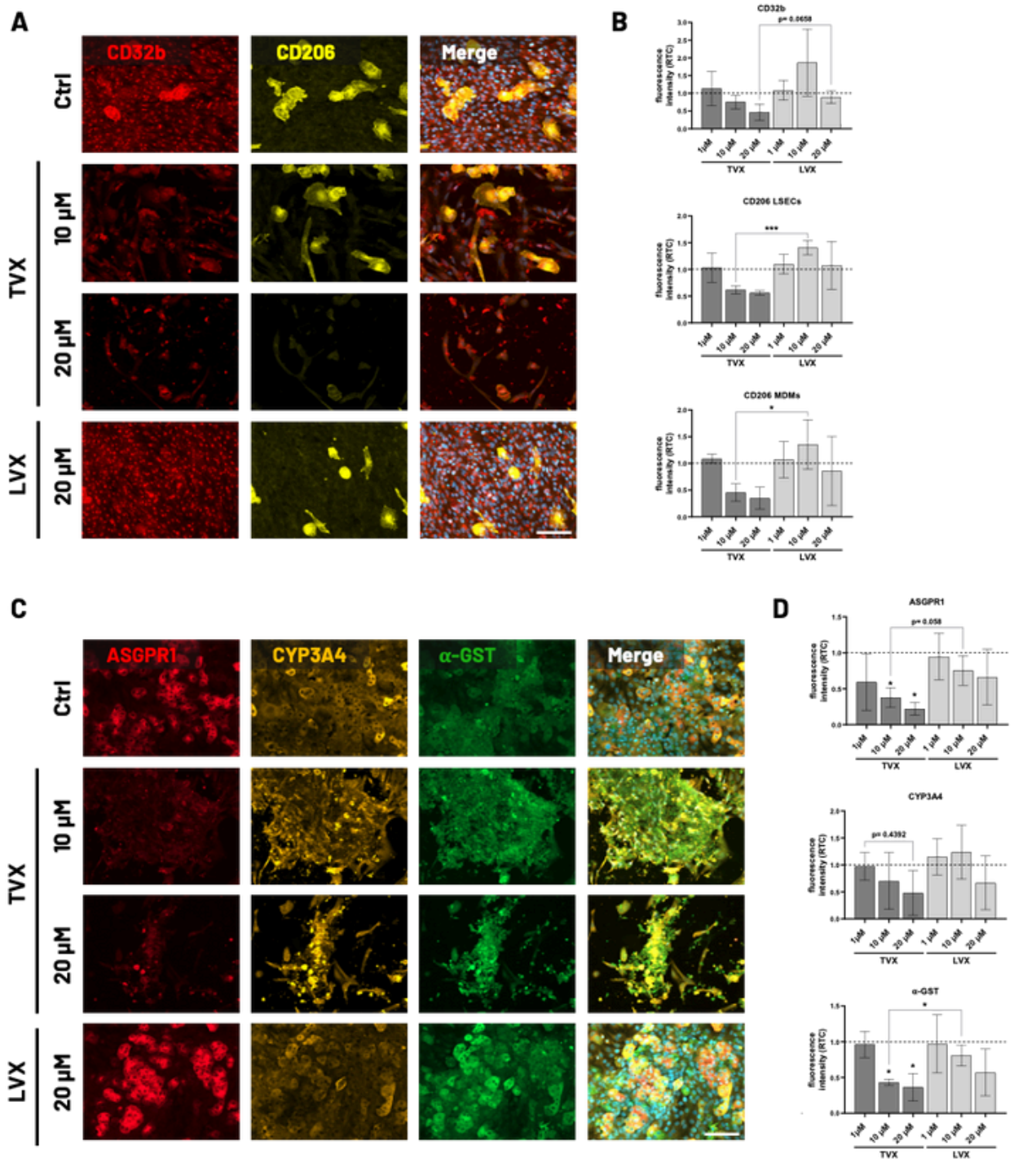

Figure 3: Morphological analysis of vascular and hepatic cell layers in the liver model. A) Representative immunofluorescence images of vascular layers (LSECs/ MDMs) stained for CD32b (red), CD206 (yellow), and nuclei (DAPI, blue in merge image) after treatment with control (Ctrl, 0.1% DMSO), TVX and LVX at a concentration of 1 µM, 10 µM or 20 µM for 7 days. Scale bar, 100 µm. B) Signal quantification of CD32b, CD206 LSECs, and CD206 MDMs fluorescence intensities. Bars show fluorescence intensity plotted as ratio to control (RTC, dotted baseline) and represent mean ± SD of 3 independent experiments (n = 3 with 5 randomly selected membrane regions for each condition). *p ≤ 0.05, ***p ≤ 0.001 (One-way ANOVA with Dunnett's multiple comparison test, two-tailed t test for comparison between indicated conditions). C) Representative immunofluorescence images of hepatic layers (HepaRG) stained for ASGPR1 (red), CYP3A4 (orange), α-GST (green), and nuclei (DAPI, blue in merge image) after treatment with control (Ctrl, 0.1% DMSO), TVX and LVX at a concentration of 1 µM, 10 µM or 20 µM for 7 days. Scale bar, 100 µm. D) Signal quantification of ASGPR1, CYP3A4, and α-GST fluorescence intensities. Bars show fluorescence intensity plotted as ratio to control (RTC, dotted baseline) and represent mean ± SD of 3 independent experiments (n = 3 with 5 randomly selected membrane regions for each condition). *p ≤ 0.05 (One-way ANOVA with Dunnett's multiple comparison test, two-tailed t test for comparison between indicated conditions).

In hepatic layers, TVX induced marked toxicity at concentrations ≥10 µM, leading to the loss of tissue integrity and delocalization of ASGPR1, CYP3A4, and α-GST signals (Figure 3 C-D). TVX significantly reduced ASGPR1 and α-GST intensities, while CYP3A4 levels showed a downward trend. Although LVX slightly reduced fluorescence intensities of ASGPR1, CYP3A4, and α-GST, it did not alter tissue morphology or integrity.

4. Detection of clinical parameters of liver toxicity in the microphysiological model

Liver models were treated with TVX and LVX and collected medium supernatants from both the vascular and hepatic biochip channels were analyzed for the release of LDH, ALT, and inflammatory cytokines. TVX treatment, especially at 20 µM, led to a concentration-dependent increase in LDH levels in the vascular compartment after 48 h and 72 h (Figure 4 A), with the peak LDH release observed at 48 h. LVX treatment did not elevate LDH levels. ALT, a clinical marker for hepatocellular injury, was further evaluated. Treatment with 20 µM TVX resulted in a significant increase in ALT release in the vascular chamber after 72 h (Figure 4B), showing hepatocyte-specific toxicity. LVX did not significantly affect ALT levels, thereby differentiating its safety profile from TVX. In addition to these markers of cell damage, inflammatory responses were measured by quantifying cytokine release from vascular supernatants. TVX treatment, particularly at 10 µM and 20 µM, caused a marked increase in pro-inflammatory cytokines, including IL-18 and IL-8, after 48 h and 72 h (Figure 4 C). Moreover, TVX at 20 µM also led to elevated IL-1β levels and a significant decrease in IL-6 (data not shown), contrasting with LVX, which did not trigger substantial changes in cytokine release.

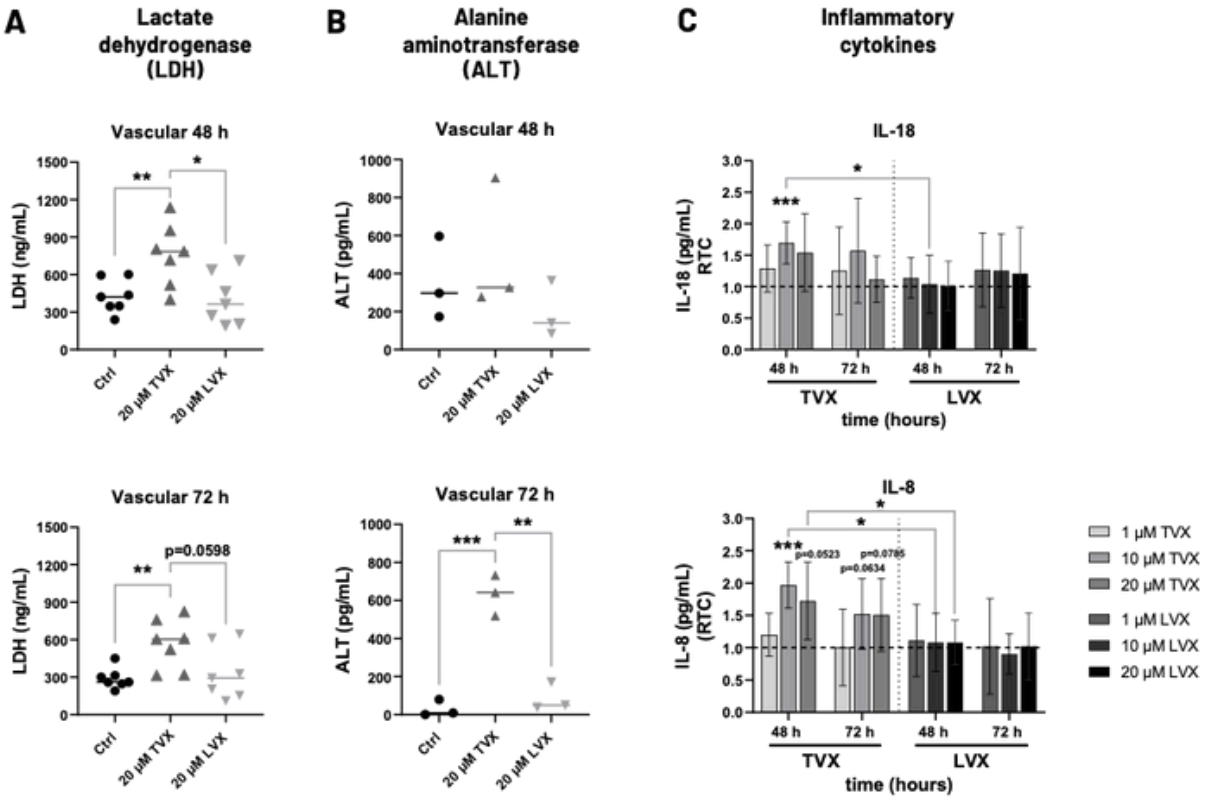

Figure 4: Measurement of liver injury markers. A) Comparison of LDH release in vascular supernatants 48 h and 72 h after treatment with TVX or LVX (20 µM). The quantified LDH concentration (ng/mL) was plotted as mean ± SD of at least 5 independent experiments (n ≥ 5). *p ≤ 0.05, **p ≤ 0.01 (Two-tailed t test). B) Comparison of ALT release in vascular supernatants 48 h and 72 h after treatment with TVX or LVX (20 µM). The quantified ALT concentration (pg/mL) was plotted as mean ± SD of 3 independent experiments (n = 3). *p ≤ 0.05, **p ≤ 0.01, ***p ≤ 0.001 (Two-tailed t test). C) Cytokine release in vascular supernatants of the liver model. Cytokines were measured after treatment with control (Ctrl, 0.1% DMSO), 1 µM, 10 µM, 20 µM of TVX or LVX for 48 h and 72 h. Bars indicate cytokine concentrations (pg/mL) plotted as ratio to control (RTC, dotted baseline) and represent mean ± SD of at least 4 independent biochip experiments with at least 3 different MDM donors (n ≥ 4). *p ≤ 0.05, ***p ≤ 0.001 (Multiple t tests with Holm-Sidak's multiple comparison test).

5. Examination of glutathione depletion and mitochondrial reactive oxygen species (ROS) formation as TVX-mediated toxicity mechanisms

Recent findings have demonstrated that mitochondrial ROS formation plays a key role in TVX-induced hepatotoxicity (Hsiao et al., 2010). In the microphysiological liver model, treatment with 10 µM and 20 µM TVX resulted in a significant reduction in intracellular glutathione in HepaRG cells, with mBCI signal intensity decreasing by 39% and 68% compared to control-treated models (Figure 5 A-B). Additionally, TVX caused a concentration-dependent trend of decrease in MitoTracker signal intensity, most pronounced at 20 µM, indicating mitochondrial dysfunction. TVX treatment further led to an increase in mitochondrial ROS, with a 2.5-fold rise at 10 µM and a fourfold rise at 20 µM, compared to control models. This ROS production was significantly higher in TVX-treated models than in those treated with LVX. These results highlight that TVX induces oxidative stress and mitochondrial damage, leading to hepatotoxicity, while LVX exhibits minimal impact on these pathways.

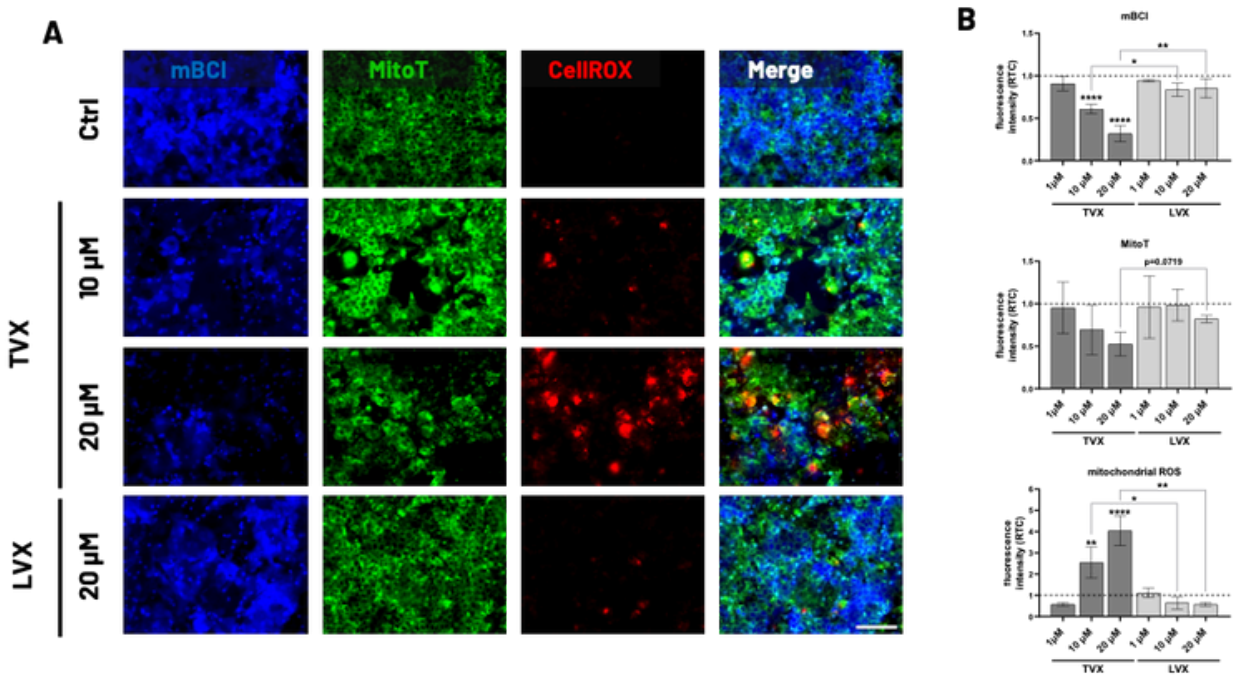

Figure 5: Live cell staining of glutathione and mitochondrial ROS formation in the liver model. A) Representative images of glutathione (mBCI, blue), mitochondrial integrity (MitoT, MitoTracker, green) and ROS formation (CellROX, red) after treatment with control (Ctrl, 0.1% DMSO), 1 µM, 10 µM and 20 µM TVX or LVX for 72 h in the liver model. Scale bar, 100 µm. B) Fluorescence signal quantification of mBCI, MitoTracker and mitochondrial ROS. Bars show fluorescence intensity plotted as ratio to control (RTC, dotted baseline) and represent mean ± SD of 3 independent experiments (n = 3 with 5 randomly selected membrane regions for each condition). *p ≤ 0.05, **p ≤ 0.01, ****p ≤ 0.0001 (One-way ANOVA with Dunnett's multiple comparison test, two-tailed t test for comparison between indicated condition.

Conclusion

This study investigated the hepatotoxic potential of TVX compared to the non-toxic analogue LVX at human therapeutic concentrations using a human *in vitro* microphysiological liver model. While preclinical animal studies failed to show TVX-induced liver injury independent of co-stimulatory cytokines or bacterial endotoxin (Shaw et al., 2007, 2009) this liver-on-chip model successfully demonstrated TVX hepatotoxicity, revealing significant impairments in both hepatic and vascular tissue without co-stimulation. TVX toxicity was linked to increased levels of liver damage markers (LDH, ALT), pro-inflammatory cytokines, and mitochondrial oxidative stress, independent of external stimulation (e.g., LPS or TNF-α). Notably, these toxic effects were not observed in LVX treatment.

The study highlights the value of the 3D liver model in replicating complex multicellular interactions and revealing intrinsic and immunomodulatory toxicity mechanisms of TVX. By incorporating LSECs and MDMs, the model advanced earlier liver models, capturing both direct hepatocellular and vascular injury. Interestingly, the immune response appeared to be modulated by hepatocytes and LSECs rather than solely dependent on MDMs, underscoring the model's ability to explore cellular crosstalk during DILI.

Further, TVX treatment triggered mitochondrial dysfunction, reduced glutathione, and increased reactive oxygen species (ROS), adding evidence for TVX-induced mitochondrial impairment.

In conclusion, the study affirms the utility of this human liver model in preclinical testing for hepatotoxicity, especially for drugs like TVX that display DILI risks in humans but not in rodent models.

Key takeaways

- The microphysiological liver model detected DILI induced by TVX at therapeutic concentrations and was able to demonstrate intrinsic toxicity mechanisms.
- TVX-induced liver injury involved interactions between hepatocytes, LSECs, and MDMs, emphasizing the need for complex cell models.
- The human liver model identified TVX toxicity more accurately compared to rodent models, suggesting a more predictive approach for DILI testing.

References

Stevens, J. L., & Baker, T. K. (2009). The future of drug safety testing: Expanding the view and narrowing the focus. Drug Discovery Today, 14(3), 162–167. https://doi.org/10.1016/j.drudis.2008.11.009

Watkins, P. (2011). Drug Safety Sciences and the Bottleneck in Drug Development. Clinical Pharmacology & Therapeutics, 89(6), 788–790. https://doi.org/10.1038/clpt.2011.63

Andrade, R. J., Lucena, M. I., Fernández, M. C., Pelaez, G., Pachkoria, K., García-Ruiz, E., García-Muñoz, B., González-Grande, R., Pizarro, A., Durán, J. A., Jiménez, M., Rodrigo, L., Romero-Gomez, M., Navarro, J. M., Planas, R., Costa, J., Borras, A., Soler, A., Salmerón, J., & Martin-Vivaldi, R. (2005). Drug-Induced Liver Injury: An Analysis of 461 Incidences Submitted to the Spanish Registry Over a 10-Year Period. Gastroenterology, 129(2), 512–521. https://doi.org/10.1053/j.gastro.2005.05.006

Chalasani, N., Bonkovsky, H. L., Fontana, R., Lee, W., Stolz, A., Talwalkar, J., Reddy, K. R., Watkins, P. B., Navarro, V., Barnhart, H., Gu, J., Serrano, J., Ahmad, J., Bach, N., Bansal, M., Barnhart, H. X., Beavers, K., Bonkovsky, H., Calvo, F. O., … Van Raaphorst, R. (2015). Features and Outcomes of 899 Patients With Drug-Induced Liver Injury: The DILIN Prospective Study. Gastroenterology, 148(7), 1340-1352.e7. https://doi.org/10.1053/j.gastro.2015.03.006

Ball, P., Mandell, L., Niki, Y., & Tillotson, G. (1999). Comparative Tolerability of the Newer Fluoroquinolone Antibacterials. Drug Safety, 21(5), 407–421. Stevens, J. L., & Baker, T. K. (2009). The future of drug safety testing: Expanding the view and narrowing the focus. Drug Discovery Today, 14(3), 162–167. https://doi.org/10.1016/j.drudis.2008.11.009

De Sarro, A., & De Sarro, G. (2001). Adverse reactions to fluoroquinolones. An overview on mechanistic aspects. Curr Med Chem, 8(4), 371–384. PubMed. https://doi.org/10.2174/0929867013373435

Olson, H., Betton, G., Robinson, D., Thomas, K., Monro, A., Kolaja, G., Lilly, P., Sanders, J., Sipes, G., Bracken, W., Dorato, M., Van Deun, K., Smith, P., Berger, B., & Heller, A. (2000). Concordance of the Toxicity of Pharmaceuticals in Humans and in Animals. Regulatory Toxicology and Pharmacology, 32(1), 56–67. https://doi.org/10.1006/rtph.2000.1399

Butler, L. D., Guzzie-Peck, P., Hartke, J., Bogdanffy, M. S., Will, Y., Diaz, D., Mortimer-Cassen, E., Derzi, M., Greene, N., & DeGeorge, J. J. (2017). Current nonclinical testing paradigms in support of safe clinical trials: An IQ Consortium DruSafe perspective. Current Nonclinical Testing Paradigms in Support of Safe Clinical Trials: An IQ Consortium DruSafe Perspective, 87, S1–S15. https://doi.org/10.1016/j.yrtph.2017.05.009

Rennert, K., Steinborn, S., Gröger, M., Ungerböck, B., Jank, A.-M., Ehgartner, J., Nietzsche, S., Dinger, J., Kiehntopf, M., Funke, H., Peters, F. T., Lupp, A., Gärtner, C., Mayr, T., Bauer, M., Huber, O., & Mosig, A. S. (2015). A microfluidically perfused three dimensional human liver model. Biomaterials, 71, 119–131. https://doi.org/10.1016/j.biomaterials.2015.08.043

Hsiao, C.-J. J., Younis, H., & Boelsterli, U. A. (2010). Trovafloxacin, a fluoroquinolone antibiotic with hepatotoxic potential, causes mitochondrial peroxynitrite stress in a mouse model of underlying mitochondrial dysfunction. Chemico-Biological Interactions, 188(1), 204–213. https://doi.org/10.1016/j.cbi.2010.07.017

Shaw, P. J., Hopfensperger, M. J., Ganey, P. E., & Roth, R. A. (2007). Lipopolysaccharide and Trovafloxacin Coexposure in Mice Causes Idiosyncrasy-Like Liver Injury Dependent on Tumor Necrosis Factor-Alpha. Toxicological Sciences, 100(1), 259–266. https://doi.org/10.1093/toxsci/kfm218

Shaw, P. J., Beggs, K. M., Sparkenbaugh, E. M., Dugan, C. M., Ganey, P. E., & Roth, R. A. (2009). Trovafloxacin enhances TNF-induced inflammatory stress and cell death signaling and reduces TNF clearance in a murine model of idiosyncratic hepatotoxicity. Toxicological Sciences: An Official Journal of the Society of Toxicology, 111(2), 288–301. https://doi.org/10.1093/toxsci/kfp163

DYNAMIC42

Get in touch

Email
info@dynamic42.com

Web
dynamic42.com

Join us

Head Office
+49 (0) 3641 508101

Dynamic42 GmbH
Winzerlaer Straße 2
07745 Jena
Germany